

## In Vivo Imaging of Near-Membrane Calcium Ions with Two-Photon Probes

Chang Su Lim, Min Young Kang, Ji Hee Han, Isravel Antony Danish, and Bong Rae Cho\*<sup>[a]</sup>

*Dedicated to Professor Eun Lee on the occasion of his retirement and 65th birthday*

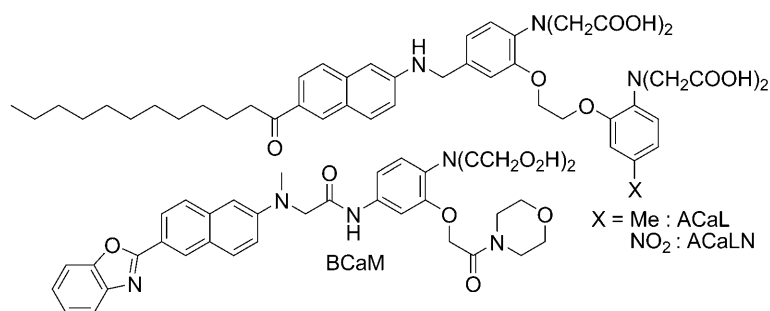
**Abstract:** We report a two-photon (TP) probe (ACaLN) for near-membrane  $\text{Ca}^{2+}$  that shows a 13-fold TP excited fluorescence (TPEF) enhancement in response to  $\text{Ca}^{2+}$ , dissociation constants ( $K_d^{\text{TP}}$ ) of  $(1.9 \pm 0.2) \mu\text{M}$ , pH-insensitivity at the biologically relevant pH, and can detect near-membrane  $\text{Ca}^{2+}$  in live cells for more than 1500 s and in living tissues at 120  $\mu\text{m}$  depth without interference from other metal ions. Comparison with existing probes provides a useful strategy for the design of efficient TP probes for the near-membrane metal ions.

**Keywords:** calcium • fluorescence • nonlinear spectroscopy • microscopy • two-photon probe

### Introduction

Calcium ions ( $\text{Ca}^{2+}$ ) play a pivotal role in the physiology and biochemistry of organisms and cells.<sup>[1,2]</sup> In mammals, calcium levels are tightly regulated with bone acting as the major mineral storage site.  $\text{Ca}^{2+}$  is released from bone into the bloodstream under controlled conditions. There is a very large transmembrane electrochemical gradient of  $\text{Ca}^{2+}$  driving the entry of  $\text{Ca}^{2+}$  into cells.<sup>[1]</sup> As the cytosolic free  $\text{Ca}^{2+}$  ( $[\text{Ca}^{2+}]_c$ ) must be kept low, the excess  $\text{Ca}^{2+}$  is extruded out of the cells.<sup>[1]</sup> Transport of the  $\text{Ca}^{2+}$  into and out of the cells functions as a signal for numerous cellular processes such as fertilization, cell death, sensory transduction, muscle contraction, and fluid secretion.<sup>[1,2]</sup> Also, many physiologi-

cal functions, including exocytosis, control of membrane  $\text{K}^+$  and  $\text{Ca}^{2+}$  permeability, and enzyme activity, are regulated by the near-membrane  $\text{Ca}^{2+}$  concentration ( $[\text{Ca}^{2+}]_m$ ). To understand the biological functions of  $[\text{Ca}^{2+}]_m$ , it is crucial to monitor the translocation of  $\text{Ca}^{2+}$  across the plasma membrane. For this purpose, we have developed a few two-photon (TP) probes (ACaL, ACaCL, and BCaM).<sup>[3]</sup> These



probes were far superior to the existing one-photon (OP) fluorescent probes, such as  $\text{C}_{18}$ -Fura-2 and Calcium Green  $\text{C}_{18}$ , for application in two-photon microscopy (TPM).<sup>[4]</sup> TPM, which utilizes two photons of lower energy for the excitation, has become a vital tool in biology and medicine owing to the capability of imaging deep inside tissue with tightly localized emission.<sup>[5]</sup> However, the dissociation constants ( $K_d$ ) of ACaL and ACaCL are in the order of 0.04–0.06  $\mu\text{M}$ , whereas that of BCaM is 90  $\mu\text{M}$ .<sup>[3]</sup> As  $[\text{Ca}^{2+}]_m$  varies

[a] C. S. Lim,<sup>+</sup> M. Y. Kang,<sup>+</sup> J. H. Han, Dr. I. A. Danish, Prof. Dr. B. R. Cho  
Department of Chemistry  
Korea University  
1-Anamdong, Seoul, 136-701 (Korea)  
Fax: (+82)2-3290-3544  
E-mail: chobr@korea.ac.kr

[<sup>+</sup>] These two authors contributed equally to this work.

Supporting information for this article is available on the WWW under <http://dx.doi.org/10.1002/asia.201100156>.

depending on the cell types and cell functions, there is a need to develop TP probes with a variety of  $K_d$  values.

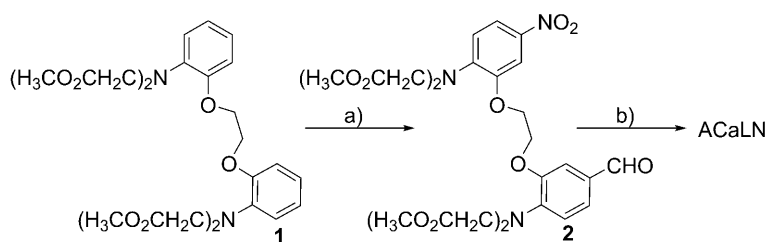
In this context, we have developed a new TP probe for near-membrane  $\text{Ca}^{2+}$  derived from 2-amino-6-dodecanoylnaphthalene (L) as the reporter (ACaLN), and *p*-nitro derivative of *O,O'*-bis(2-aminophenyl)ethyleneglycol-*N,N,N',N'*-tetraacetic acid (NBAPTA) as the  $\text{Ca}^{2+}$  receptor. NBAPTA is a well-known  $\text{Ca}^{2+}$  chelator that has been employed in one-photon fluorescent probes, such as Calcium Green-5N and Orgon Green 488 BAPTA-5N,<sup>[6]</sup> while L is a TP polarity probe that has been widely used as a membrane probe.<sup>[7]</sup> Herein, we report that ACaLN shows a moderate  $K_d$  value (2  $\mu\text{M}$ ) and can detect near-membrane  $\text{Ca}^{2+}$  in live cells and tissues at >100  $\mu\text{m}$  depth by TPM without interference from competing metal ions, pH, and mistargeting and photobleaching problems.

## Results and Discussion

Synthesis of ACaLN is summarized in Scheme 1. Compound **1** was prepared according to the literature method<sup>[8]</sup> and 2-amino-6-dodecanoylnaphthalene was obtained using the same method as previously reported.<sup>[3a]</sup> Compound **2** was prepared by formylation of **1** and subsequent nitration. ACaLN was prepared in 46% yield by the reductive amination between **2** and 2-amino-6-dodecanoylnaphthalene followed by hydrolysis.

The solubility of ACaLN in 3-(*N*-morpholino)propanesulfonic acid (MOPS) buffer solution (30 mM, pH 7.2) was greater than 15  $\mu\text{M}$ , which is sufficient to stain the cells (Figure S1, see the Supporting Information). The absorption and emission spectra of ACaLN show gradual bathochromic shifts with the solvent polarity in the order, 1,4-dioxane < DMF < EtOH < MOPS buffer (Figure S2 and Table S1 in the Supporting Information) and the shift is greater in the emission (64 nm) than in the absorption spectra (4 nm), thus indicating the utility of ACaLN as a polarity probe.

When  $\text{Ca}^{2+}$  was added to ACaLN in MOPS buffer solution (30 mM, pH 7.2), the fluorescence intensity increased gradually with the metal ion concentration without affecting the absorption spectra (Figures 1 a, S3, and S4 in the Supporting Information), presumably because of the blocking of the photo-induced electron transfer (PeT) process by the metal ion complexation.<sup>[5]</sup> The fluorescence enhancement



Scheme 1. Synthesis of ACaLN. a) 1)  $\text{POCl}_3$ , DMF; 2)  $\text{HNO}_3$ , AcOH,  $\text{Ac}_2\text{O}$ ; b) 1) 2-amino-6-dodecanoylnaphthalene,  $\text{NaBH}(\text{OAc})_3$ , EtOAc,  $\text{CH}_2\text{Cl}_2$ ; 2) KOH, EtOH.

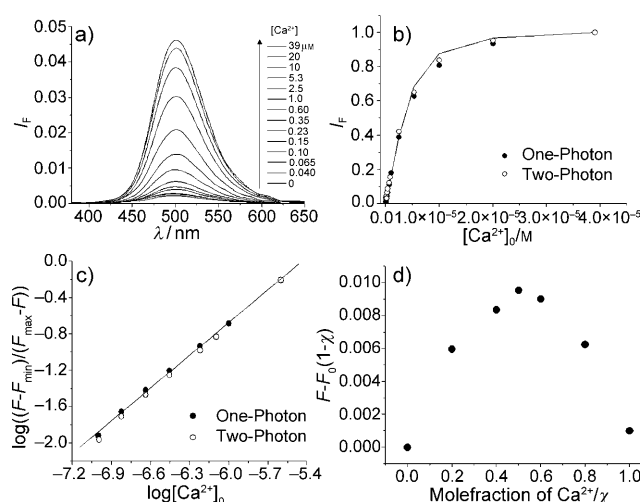


Figure 1. One-photon emission spectra (a) and one- (●) and two-photon (○) fluorescence titration curves (b) of ACaLN (3  $\mu\text{M}$ ) in the presence of various concentrations of free  $\text{Ca}^{2+}$  ions (0–39  $\mu\text{M}$ ). c) Hill plots for the complexation of ACaLN with  $\text{Ca}^{2+}$  (0–39  $\mu\text{M}$ ) measured by one- (●) and two-photon (○) spectroscopy. d) Job plot for determination of the stoichiometry of ACaLN- $\text{Ca}^{2+}$  in MOPS buffer (30 mM, pH 7.2). The total concentration of  $\text{Ca}^{2+}$  was 10  $\mu\text{M}$ . These data were measured in 30 mM MOPS, 100 mM KCl, 10 mM EGTA, pH 7.2. The excitation wavelengths for one- and two-photon processes are 365 and 750 nm, respectively.

factor [ $\text{FEF} = (F - F_{\text{min}})/F_{\text{min}}$ ] of ACaLN, measured by the one- and two-photon titration curves, is 13 in the presence of 39  $\mu\text{M}$   $\text{Ca}^{2+}$ , indicating a high sensitivity to the change in the  $\text{Ca}^{2+}$  concentration (Figure 1 a). Moreover, the titration curve fitted well with the 1:1 binding model (Figure 1 b), the Hill plots were linear with a slope of 1.0 (Figure 1 c), and the Job plot exhibited a maximum point at a mole fraction of 0.50 (Figure 1 d), thereby indicating 1:1 complexation between the probe and  $\text{Ca}^{2+}$ .<sup>[9]</sup>

The dissociation constants ( $K_d$ ) were calculated from the fluorescence titration curves (Figure 1 b).<sup>[10,11]</sup> The  $K_d$  values of ACaLN for  $\text{Ca}^{2+}$  in MOPS buffer solution as determined by one- ( $K_d^{\text{OP}}$ ) and two-photon ( $K_d^{\text{TP}}$ ) processes are  $2.1 \pm 0.4$  and  $1.9 \pm 0.2$   $\mu\text{M}$ , respectively. For comparison, the  $K_d^{\text{TP}}$  value of ACaL is 0.041.<sup>[3a]</sup> The larger  $K_d$  value for ACaLN can be attributed to the nitro group in the BAPTA which may reduce the binding ability. Moreover, the  $K_d^{\text{TP}}$  value of BCaM is 90  $\mu\text{M}$ .<sup>[3c]</sup> Therefore, we now have a series of near-membrane TP probes for  $\text{Ca}^{2+}$  with  $K_d^{\text{TP}}$  values ranging from 0.05 to 90  $\mu\text{M}$ . This allows the detection of near-membrane  $\text{Ca}^{2+}$  concentrations ranging from sub- $\mu\text{M}$  to  $\mu\text{M}$  to sub-mm.

ACaLN showed a high selectivity for  $\text{Ca}^{2+}$ , as revealed by the negligible fluorescence intensity in the presence of 2 mM concentrations of  $\text{Mg}^{2+}$ , 100  $\mu\text{M}$  of  $\text{Fe}^{2+}$ ,  $\text{Mn}^{2+}$ ,  $\text{Co}^{2+}$ ,  $\text{Cu}^{2+}$ , and  $\text{Zn}^{2+}$  and a large en-

hancement in the fluorescence intensity upon addition of 39  $\mu\text{M}$  of  $\text{Ca}^{2+}$  (Figure 2a). Hence, this probe can detect the intracellular free  $\text{Ca}^{2+}$  with minimum interference from other competing metal ions. Moreover, it was pH-insensitive at  $\text{pH} > 6.5$  (Figure 2b).

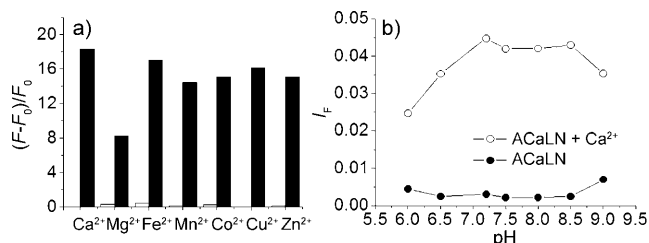


Figure 2. a) The relative fluorescence intensity of  $5 \mu\text{M}$  ACaLN in the presence of 2 mM for  $\text{Mg}^{2+}$ ; 100  $\mu\text{M}$  for  $\text{Fe}^{2+}$ ,  $\text{Mn}^{2+}$ ,  $\text{Co}^{2+}$ ,  $\text{Cu}^{2+}$ ,  $\text{Zn}^{2+}$  (empty bars) followed by addition of  $39 \mu\text{M}$   $\text{Ca}^{2+}$  (filled bar). b) Effect of the pH on the fluorescence intensity of  $3 \mu\text{M}$  ACaLN in the presence of 0 (●) and  $39 \mu\text{M}$  (○) of  $\text{Ca}^{2+}$ . These data were measured in 30 mM MOPS buffer (100 mM KCl, 10 mM EGTA, pH 7.2).

The TP action spectrum of the  $\text{Ca}^{2+}$  complexes with ACaLN in buffer solution indicated a two-photon action cross section ( $\Phi\delta$ ) value of 20 GM at 750 nm (Table 1). The value is smaller than that of ACaCL ( $\Phi\delta = 90$  GM), apparently because of the smaller  $\Phi$  value for ACaLN- $\text{Ca}^{2+}$  (0.043 vs. 0.018). The nitro group in the receptor appears to have quenched the fluorescence significantly. Nevertheless, the TPM images of cells and tissues labeled with ACaLN were bright enough to detect near-membrane  $\text{Ca}^{2+}$  by TPM (Figure 3).

To demonstrate the utility of this probe, we obtained the TPM image of cultured HT22 cells (clonal mouse hippocampal cell) labeled with  $3 \mu\text{M}$  ACaLN (Figure 3a). The image was bright and revealed the  $\text{Ca}^{2+}$  distribution in the plasma membrane. We then monitored the TPEF intensity in the ACaLN-labeled HT22 cells after addition of histamine, an agonist that stimulates the cells to release  $[\text{Ca}^{2+}]_c$  from intracellular stores, such as the endoplasmic reticulum (ER).<sup>[12]</sup> It was expected that the excess  $[\text{Ca}^{2+}]_c$  liberated by histamine would be extruded out of the cell through the cell membrane to maintain the  $\text{Ca}^{2+}$  homeostasis, thereby increasing the  $[\text{Ca}^{2+}]_m$ .<sup>[12]</sup> Indeed, the TPEF intensities in the

cell membrane began to rise after addition of histamine (100  $\mu\text{M}$ ), reached a peak value after 150 s, and returned to the baseline level after 300 s. When the cells were treated with 2 mM  $\text{CaCl}_2$ , the  $[\text{Ca}^{2+}]_m$  increased immediately, reached a maximum intensity after 50 s, and then decreased to the baseline level after 10 min (Figure 3b).<sup>[12]</sup> Hence, ACaLN is clearly capable of monitoring the changes in  $[\text{Ca}^{2+}]_m$  in live cells over a long time period.

We further investigated the utility of this probe in tissue imaging. TPM images were obtained from a section of a fresh rat hippocampal slice incubated with  $30 \mu\text{M}$  ACaLN for 30 min at  $37^\circ\text{C}$ . The bright-field image reveals the CA1 and CA3 regions as well as the dentate gyrus (DG, Figure 3c). As the structure of the brain tissue is known to be inhomogeneous in its entire depth, we accumulated 10 TPM images at depths of 90–180  $\mu\text{m}$  to visualize the distributions of the  $[\text{Ca}^{2+}]_m$ . The accumulated TPM image shows that the  $[\text{Ca}^{2+}]_m$  is more abundant in the CA1 than in the DG and CA3 regions (Figure 3d). The TPM image obtained at a higher magnification clearly reveals  $\text{Ca}^{2+}$  distribution in the cell membrane at 120  $\mu\text{m}$  depth in live tissue (Figure 3e). Moreover, when ethylene diamine tetraacetic acid (EDTA), a membrane-permeable  $\text{Ca}^{2+}$  chelator that can effectively remove  $\text{Ca}^{2+}$ , was added to the imaging solution, the TPEF intensity decreased (Figure 3h). Further, the TPM images of the slices labeled with ACaLN revealed the  $[\text{Ca}^{2+}]_m$  distribution in the given  $xy$  plane at 90–180  $\mu\text{m}$  depth, indicating the sectioning capability of TPM (Figure S7 in the Supporting Information). These findings demonstrate that ACaLN is capable of detecting membrane  $\text{Ca}^{2+}$  at 120  $\mu\text{m}$  depth in live tissues using TPM.

It is noteworthy that the TPM image of the ACaLN-labeled tissue reveals the distribution of  $[\text{Ca}^{2+}]_m$  over the entire cell membranes deep inside intact tissue, while those labeled with ACaCL and BCaM show intense and dim regions, respectively. This outcome suggests that the  $K_d$  value of ACaLN is similar to  $[\text{Ca}^{2+}]_m$ , whereas that of ACaCL is too small and emits strong TPEF in the regions where  $[\text{Ca}^{2+}]_m \gg 0.05 \mu\text{M}$ , and that of BCaM is too large and emits little TPEF in the region where  $[\text{Ca}^{2+}]_m \ll 90 \mu\text{M}$ . Notably, low and high affinity probes can highlight the  $[\text{Ca}^{2+}]_m$ -rich regions. This result underlines the importance of developing TP probes for  $[\text{Ca}^{2+}]_m$  with a variety of  $\text{Ca}^{2+}$  ion affinities.

Moreover, the image with BCaM is not as clear as those with ACaL and ACaLN and reveals blurred domains where the probes appear to be aggregated, indicating that a long chain hydrocarbon is crucial for the staining the cell membranes deep inside intact tissue.

Table 1. Photophysical data for ACaL, ACaLN, and BCaM.<sup>[a]</sup>

Compound <sup>d</sup>	$\lambda_{\text{max}}^{(1)}/\lambda_{\text{max}}^{(2)}$ [b]	$\Phi$ [c]	$K_d^{\text{OP}}/K_d^{\text{TP}}$ [d]	$\lambda_{\text{max}}^{(2)}$ [e]	$\Phi\delta$ [f]
ACaL [g]	369/500	0.0037		nd [h]	nd [h]
ACaL + $\text{Ca}^{2+}$ [g]	372/502	0.043	0.045/0.041	780	90
ACaLN	364/498	0.0013		nd [h]	nd [h]
ACaLN + $\text{Ca}^{2+}$	354/497	0.018	2.1/1.9	750	20
BCaM [i]	360/470	0.070		nd [h]	nd [h]
BCaM + $\text{Ca}^{2+}$ [i]	360/470	0.98	89/78	780	150

[a] All data were measured in 30 mM MOPS buffer in the absence and presence (39  $\mu\text{M}$ ) of free  $\text{Ca}^{2+}$ . [b]  $\lambda_{\text{max}}$  of the one-photon absorption and emission spectra in nm. [c] Fluorescence quantum yield. The uncertainty is  $\pm 10\%$ . [d] Dissociation constants for  $\text{Ca}^{2+}$  in  $\mu\text{M}$  measured by one- ( $K_d^{\text{OP}}$ ) and two-photon ( $K_d^{\text{TP}}$ ) processes. The uncertainty is  $\pm 12\%$ . [e]  $\lambda_{\text{max}}$  of the two-photon excitation spectra in nm. [f] The two-photon action cross section in  $10^{-50} \text{ cm}^4 \text{ s/photon}$  (GM). The uncertainty is  $\pm 15\%$ . [g] Ref. [3a]. [h] Not determined because TPEF intensity was too weak to measure the TP action cross section accurately. [i] Ref. [3c].

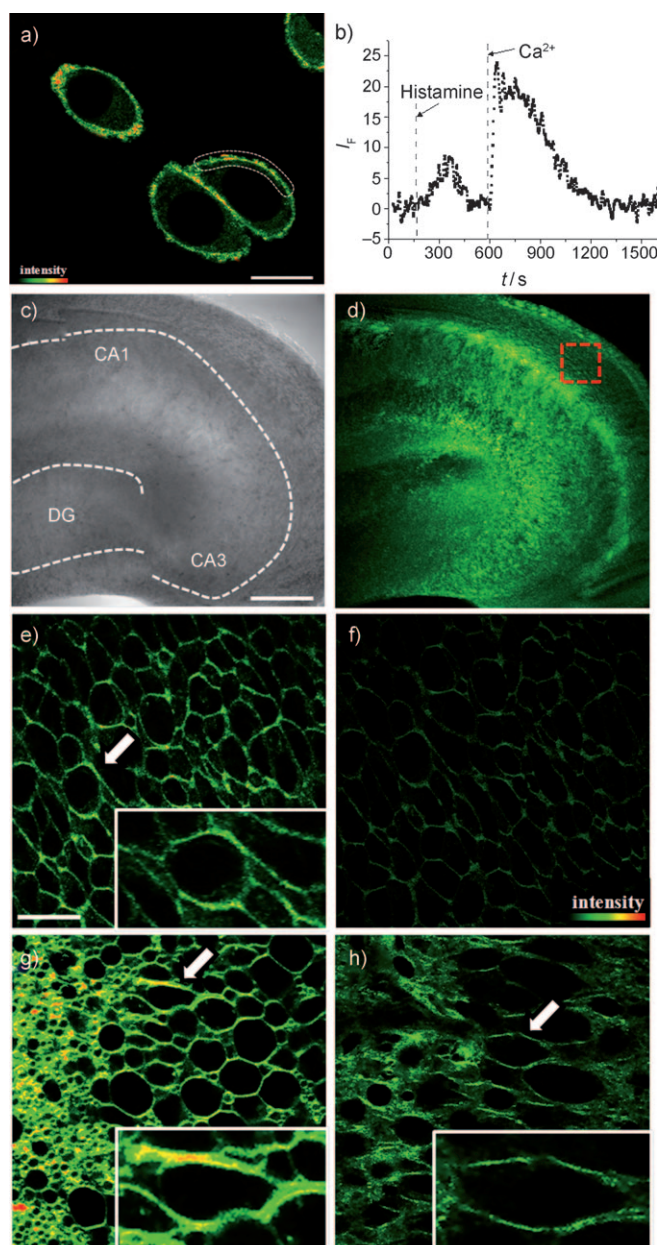


Figure 3. a) Pseudo colored two-photon microscopy (TPM) images of HT22 cells labeled with  $3\ \mu\text{M}$  ACaLN. b) Time course of two-photon excited fluorescence (TPEF) at the position marked with a dotted line in (a) after stimulation with  $100\ \text{mM}$  histamine in nominally calcium-ion-free buffer, followed by addition of  $2\ \text{mM}$   $\text{CaCl}_2$  to the imaging solution. TPEF was collected at  $360\text{--}620\ \text{nm}$  upon excitation at  $750\ \text{nm}$ . c–f) Images of a fresh rat hippocampal slice labeled with  $30\ \mu\text{M}$  ACaLN. c) Bright-field images showing the CA1 and CA3 regions as well as dentate gyrus (DG) upon  $10\times$  magnification. White dotted lines indicate the pyramidal neuron layers. d) 10 TPM images collected in (c) along the  $z$  direction at the depths of  $90\text{--}180\ \mu\text{m}$  were accumulated. e) TPM images of the red labeled region at a depth of  $\sim 120\ \mu\text{m}$  by  $100\times$  magnification. f) TPM images of the same region after addition of  $200\ \mu\text{M}$  EDTA to (e). g, h) TPM images of fresh rat hippocampal slices labeled with  $30\ \mu\text{M}$  ACaLN and BCaM, respectively. Image (g) was taken from Ref. [3a], and images (d–f) and (h) were collected at  $360\text{--}620\ \text{nm}$  upon excitation at  $750$  and  $780\ \text{nm}$ , respectively, with fs pulses. The images in the white boxes are the enlarged images of the cells indicated by the white arrows. Scale bar,  $15$  (a),  $30$  (e, f, g, h), and  $300\ \mu\text{m}$  (c, d), respectively.

## Conclusions

In conclusion, we have developed a TP probe (ACaLN) that shows a 13-fold TPEF enhancement in response to  $\text{Ca}^{2+}$ , dissociation constants ( $K_d^{\text{TP}}$ ) of  $(1.9 \pm 0.2)\ \mu\text{M}$ , pH insensitivity in the biologically relevant pH, and can detect near-membrane  $\text{Ca}^{2+}$  in live cells for more than  $1500\ \text{s}$  and in living tissues at  $120\ \mu\text{m}$  depth without interference from other metal ions. These results provide a useful strategy for the design of efficient TP probes for the near-membrane metal ions.

## Experimental Section

### Synthetic Materials and Methods

Silica gel P60 (SiliCycle) was used for column chromatography. All other chemicals were purchased from Sigma–Aldrich and were used as received.

### Compound 2

A mixture of  $\text{POCl}_3$  ( $3.2\ \text{mL}$ ,  $34\ \text{mmol}$ ) and  $N,N$ -dimethylformamide (DMF;  $6\ \text{mL}$ ) was stirred at  $0^\circ\text{C}$  for  $1\ \text{h}$ . This mixture was added to the solution of **1** ( $6.0\ \text{g}$ ,  $11\ \text{mmol}$ ) in DMF ( $30\ \text{mL}$ ) at  $0^\circ\text{C}$  and heated to  $60^\circ\text{C}$  for  $30\ \text{min}$ . The crude product was cooled, transferred to a beaker, neutralized with  $\text{NaHCO}_3$  (aq), and extracted with ethyl acetate. The solvent was evaporated and the crude product was purified by column chromatography using hexane/EtOAc (1:1) as the eluent. Yield:  $4.8\ \text{g}$  (76%); m.p.:  $139^\circ\text{C}$ ; IR(KBr):  $\tilde{\nu}=2955, 1751, 1686\ \text{cm}^{-1}$ ;  $^1\text{H NMR}$  ( $300\ \text{MHz}$ ,  $\text{CDCl}_3$ ):  $\delta=9.78$  (1H, s),  $7.41\text{--}7.37$  (2H, m),  $6.91\text{--}6.80$  (4H, m),  $6.78$  (1H, d,  $J=8.4\ \text{Hz}$ ),  $4.28$  (4H, s),  $4.24$  (4H, s),  $4.15$  (4H, s),  $3.55$  (6H, s),  $3.54$  ppm (6H, s). This compound ( $0.50\ \text{g}$ ,  $0.89\ \text{mmol}$ ) was dissolved in acetic anhydride ( $30\ \text{mL}$ ) and stirred under ice cold conditions. A solution of  $70\%$  nitric acid ( $0.063\ \text{mL}$ ,  $0.98\ \text{mmol}$ ) in acetic acid ( $5\ \text{mL}$ ) was slowly added for  $3\ \text{h}$ . After the addition was over, the mixture was further stirred for  $1\ \text{h}$  and the reaction was quenched by dilute  $\text{NaHCO}_3$  (aq). The product was extracted with ethyl acetate, dried over  $\text{MgSO}_4$ , and purified by column chromatography using hexane/EtOAc/ $\text{CHCl}_3$  (1:1:1) as the eluent. Yield:  $0.24\ \text{g}$  (45%); m.p.:  $134^\circ\text{C}$ ; IR(KBr):  $\tilde{\nu}=2955, 1755, 1683, 1520\ \text{cm}^{-1}$ ;  $^1\text{H NMR}$  ( $300\ \text{MHz}$ ,  $\text{CDCl}_3$ ):  $\delta=9.82$  ppm (1H, s),  $\delta=7.88$  (1H, dd,  $J=9.0, 2.4\ \text{Hz}$ ),  $7.74$  (1H, d,  $J=2.4\ \text{Hz}$ ),  $7.43$  (1H, dd,  $J=7.8, 2.1\ \text{Hz}$ ),  $7.39$  (1H, d,  $J=2.1\ \text{Hz}$ ),  $6.80$  (1H, d,  $J=7.8\ \text{Hz}$ ),  $6.71$  (1H, d,  $J=9.0\ \text{Hz}$ ),  $4.33$  (4H, s),  $4.23$  (8H, s),  $3.63$  (6H, s),  $3.60$  ppm (6H, s);  $^{13}\text{C NMR}$  ( $100\ \text{MHz}$ ,  $\text{CDCl}_3$ ):  $\delta=190.4, 171.2, 170.9, 145.2, 145.1, 142.9, 142.6, 140.9, 129.9, 127.2, 118.5, 116.7, 116.0, 110.5, 107.8, 67.4, 66.8, 53.6, 53.5, 52.1, 52.0$  ppm.

### ACaLN

A mixture of 2-amino-6-dodecanoylnaphthalene ( $0.10\ \text{g}$ ,  $0.16\ \text{mmol}$ ) and **2** ( $53\ \text{mg}$ ,  $0.16\ \text{mmol}$ ) in anhydrous EtOAc ( $5\ \text{mL}$ ) was refluxed overnight. The solvent was evaporated, and  $\text{NaBH}(\text{OAc})_3$  ( $70\ \text{mg}$ ,  $0.32\ \text{mmol}$ ) in  $\text{CH}_2\text{Cl}_2$  ( $5\ \text{mL}$ ) was added, and the mixture was refluxed overnight. The product was isolated by evaporation and purified by column chromatography using hexane/EtOAc (5:1) as the eluent. Yield:  $89\ \text{mg}$  (61%). Ethanol ( $2.5\ \text{mL}$ ) and KOH in ethanol ( $1.0\ \text{M}$ ,  $0.97\ \text{mL}$ ) were added to this compound ( $89\ \text{mg}$ ,  $0.097\ \text{mmol}$ ). After stirring overnight, the volume was reduced by half, and dilute HCl (aq) was added slowly until pH 3–4 to obtain the product as an orange solid, which was washed with distilled water. Yield:  $62\ \text{mg}$  (75%); m.p.:  $159^\circ\text{C}$ ; IR(KBr):  $\tilde{\nu}=3412, 1718, 1618, 1512\ \text{cm}^{-1}$ ;  $^1\text{H NMR}$  ( $300\ \text{MHz}$ ,  $[\text{D}_4]\text{MeOH}$ ):  $\delta=8.26$  (1H, d,  $J=1.5\ \text{Hz}$ ),  $7.78\text{--}7.70$  (2H, m),  $7.64$  (1H, d,  $J=9.0\ \text{Hz}$ ),  $7.64$  (1H, d,  $J=2.4\ \text{Hz}$ ),  $7.48$  (1H, d,  $J=9.0\ \text{Hz}$ ),  $7.10\text{--}7.00$  (2H, m),  $6.92$  (1H, dd,  $J=8.1, 1.5\ \text{Hz}$ ),  $6.83$  (1H, d,  $J=8.1\ \text{Hz}$ ),  $6.73$  (1H, d,  $J=1.8\ \text{Hz}$ ),  $6.71$  (1H, d,  $J=9.0\ \text{Hz}$ ),  $4.32$  (2H, s),  $4.25$  (4H, s),  $4.20$  (4H, s),  $4.06$  (4H, s),  $3.00$  (2H, t,  $J=7.5\ \text{Hz}$ ),  $1.69$  (2H, quin,  $J=7.5\ \text{Hz}$ ),  $1.26$  (16H, m),  $0.88$  ppm (3H, t,  $J=6.9\ \text{Hz}$ );  $^{13}\text{C NMR}$  ( $100\ \text{MHz}$ ,  $[\text{D}_4]\text{MeOH}$ ):  $\delta=201.6, 174.6, 173.4, 150.5, 149.3,$

148.4, 145.5, 140.4, 138.5, 138.1, 133.6, 130.6, 130.2, 130.0, 129.7, 125.9, 125.7, 124.1, 120.2, 118.8, 118.0, 115.2, 112.8, 108.1, 103.2, 67.7, 66.7, 54.4, 46.9, 46.7, 37.9, 35.3, 33.8, 31.9, 29.6, 29.3, 26.9, 25.7, 24.9, 22.6, 13.3 ppm. HR-MS calculated for  $[M+H]^+$ : 859.3767; found: 859.3765.

#### Spectroscopic Measurements

Absorption spectra were recorded on a Hewlett-Packard 8453 diode array spectrophotometer and fluorescence spectra were obtained with Aminco-Bowman series 2 luminescence spectrometer using a 1 cm path-length standard quartz cell. The fluorescence quantum yield was determined by using Coumarin 307 as the reference using the literature method.<sup>[13]</sup>

#### Solubility of ACalN in MOPS Buffer

A small amount of dye was dissolved in DMSO to prepare the stock solutions ( $1.0 \times 10^{-3}$  M). The solution was diluted to  $6.0 \times 10^{-3}$ – $6.0 \times 10^{-5}$  M and added to a cuvette containing MOPS buffer (3.0 mL, pH 7.2) using a micro syringe. In all cases, the concentration of DMSO in H<sub>2</sub>O was maintained to be 0.2%.<sup>[3]</sup> The plots of absorbance against the dye concentration were linear at low concentration and showed downward curvature at higher concentrations (Figure S1 in the Supporting Information). The maximum concentration in the linear region was taken as the solubility. The solubility of ACalN in MOPS buffer was greater than 15  $\mu$ M.

#### Determination of Apparent Dissociation Constants

A series of solutions containing various  $[Ca^{2+}]$  were prepared in the presence of 3  $\mu$ M ACalN in 30 mM MOPS buffer and they were adjusted to pH 7.2. The apparent dissociation constant ( $K_d$ ) was determined using the following equation:  $F - F_{min} = [Ca^{2+}](F_{max} - F_{min})/(K_d + [Ca^{2+}])$ , where  $F$  is the observed fluorescence,  $F_{max}$  is the fluorescence for the  $Ca^{2+}$ -ACalN complex, and  $F_{min}$  is the fluorescence for the free ACalN. The  $K_d$  value that best fits the titration curve (Figures 2 and S3 in the Supporting Information) using the equation was calculated by using the Excel program as previously reported.<sup>[9,10]</sup> In order to determine the  $K_d^{TP}$  for the two-photon process, the TPEF intensity was recorded in the range of 400–620 nm with a CCD detector excited by a mode-locked titanium-sapphire laser source (Coherent Chameleon, 90 MHz, 200 fs) set at a wavelength of 750 nm and output power 1348 mW, which corresponded to approximately 200 mW average power in the focal plane.

#### Measurement of Two-Photon Cross Section

The two-photon cross section ( $\delta$ ) was determined by using the femtosecond (fs) fluorescence measurement technique as described previously.<sup>[14]</sup> ACalN was dissolved in 30 mM MOPS buffer (pH 7.2) at concentrations of  $5.0 \times 10^{-6}$  M and then the two-photon induced fluorescence intensity was measured at 740–900 nm using rhodamine 6G as the reference, the two-photon property of which has been well characterized in the literature.<sup>[15]</sup> The intensities of the two-photon induced fluorescence spectra of the reference and sample emitted at the same excitation wavelength were determined. The TPA cross section was calculated by using  $\delta = \delta_r (S_s \Phi_r \phi_r c_r) / (S_r \Phi_s \phi_s c_s)$ : where the subscripts  $s$  and  $r$  stand for the sample and reference molecules, respectively. The intensity of the signal collected by a CCD detector was denoted as  $S$ .  $\Phi$  is the fluorescence quantum yield.  $\phi$  is the overall fluorescence collection efficiency of the experimental apparatus. The number density of the molecules in solution was denoted as  $c$ .  $\delta_r$  is the TPA cross section of the reference molecule. The TP action cross section of ACalN was 20 GM at 750 nm.

#### Cell Culture and Imaging

HT22 clonal mouse hippocampal cells were cultured in Dulbecco's Modified Eagle's Medium (DMEM, WelGene) supplemented with heat-inactivated 10% fetal bovine serum (FBS, WelGene), penicillin (100 units mL<sup>-1</sup>), and streptomycin (100  $\mu$ g mL<sup>-1</sup>). All cells were kept in a humidified atmosphere of 5:95 (v/v) of CO<sub>2</sub>/air at 37°C. Two days before imaging, the cells were passed and plated on glass-bottomed dishes (MatTek). For labeling, the growth medium was removed and replaced with DMEM without FBS. The cells were incubated with ACalN (3  $\mu$ M)

for 5 min at 25°C. The cells were washed three times with phosphate buffered saline (PBS; Gibco) without Ca<sup>2+</sup> and Mg<sup>2+</sup> and then imaged.

#### Two-Photon Fluorescence Microscopy

Two-photon fluorescence microscopy images of ACalN-labeled cells and tissues were obtained with spectral confocal and multiphoton microscopes (Leica TCS SP2) with a  $\times 100$  (NA=1.30 OIL) and  $\times 10$  (NA=0.30 DRY) objective lens, respectively. The two-photon fluorescence microscopy images were obtained with a DM IRE2 Microscope (Leica) by exciting the probes with a mode-locked titanium-sapphire laser source (Coherent Chameleon, 90 MHz, 200 fs) set at wavelength of 750 nm and output power of 1348 mW, which corresponded to approximately 10 mW average power in the focal plane. To obtain images in the 360–460 nm and 500–620 nm ranges, internal PMTs were used to collect the signals in 8 bit unsigned 512  $\times$  512 pixels at 400 Hz scan speed.

#### Detection window

The TPEF spectrum from the ACalN-labeled cells was unsymmetrical and could be fitted to two Gaussian functions with peak maxima at 434 nm (blue curve) and 475 nm (green curve), respectively (Figure S6b in the Supporting Information). The spectra are very similar to those measured in DPPC/CHL and DOPC, which are good models for the I<sub>o</sub> and I<sub>d</sub> domains, respectively (Figure S5 in the Supporting Information). Moreover, the TPM images collected in the 360–460 and 500–620 nm ranges are nearly the same except for the brightness (Figure S6c, d in the Supporting Information). Therefore, we have detected near-membrane Ca<sup>2+</sup> with ACalN by using the detection window at 360–620 nm.

#### Preparation and Staining of Fresh Rat Hippocampal Slices

All experiments were performed in accordance with the guidelines established by the Committee of Animal Research Policy of Korea University College of Medicine. Slices were prepared from the hippocampi and the hypothalmi of 2 day-old rats (SD). Coronal slices were cut into 400  $\mu$ m-thick using a vibrating-blade microtome in artificial cerebrospinal fluid (ACSF); 138.6 mM NaCl, 3.5 mM KCl, 21 mM NaHCO<sub>3</sub>, 0.6 mM NaH<sub>2</sub>PO<sub>4</sub>, 9.9 mM D-glucose, 1 mM CaCl<sub>2</sub>, and 3 mM MgCl<sub>2</sub>. Slices were incubated with 30  $\mu$ M ACalN (or BCaM) in ACSF bubbled with 95% O<sub>2</sub> and 5% CO<sub>2</sub> for 30 min at 37°C. Slices were then washed three times with ACSF and transferred to glass-bottomed dishes (MatTek) and observed in a spectral confocal multiphoton microscope. After washing three times with ACSF, the slices were transferred to glass bottomed dishes (MatTek) and observed under a spectral confocal multiphoton microscope. To observe the effect of EDTA, a solution of EDTA in MOPS buffer (200  $\mu$ M) was added to this sample and the TPM image was obtained.

## Acknowledgements

This work was supported by the National Research Foundation (NRF) grants funded by the Korean Government (No. 2010-0018921) and Priority Research Centers Program through the NRF funded by the Ministry of Education, Science and Technology (2010-0020209). C. S. Lim, M. Y. Kang, J. H. Han, and I. A. Danish were supported by BK21 scholarship.

- [1] E. Carafoli, *Physiol. Rev.* **1991**, *71*, 129–153.
- [2] a) M. D. Bootman, M. J. Berridge, *Cell* **1995**, *83*, 675–678; b) M. D. Bootman, M. J. Berridge, P. Lipp, *Cell* **1997**, *91*, 367–373; c) M. D. Bootman, M. J. Berridge, P. Lipp, *Nature* **1998**, *395*, 645–648; d) D. E. Clapham, *Cell* **1995**, *80*, 259–268.
- [3] a) P. S. Mohan, C. S. Lim, Y. S. Tian, W. Y. Roh, J. H. Lee, B. R. Cho, *Chem. Commun.* **2009**, 5365–5367; b) Y. N. Shin, C. S. Lim, Y. S. Tian, W. Y. Rho, B. R. Cho, *Bull. Korean Chem. Soc.* **2010**, *31*, 599–605; c) H. J. Kim, J. H. Han, M. J. Kim, C. S. Lim, H. M. Kim, B. R. Cho, *Angew. Chem.* **2010**, *122*, 6938–6941; *Angew. Chem. Int. Ed.* **2010**, *49*, 6786–6789.

- [4] a) Q. P. Lloyd, M. A. Kuhn, C. V. Gay, *J. Biol. Chem.* **1995**, *270*, 22445–22451; b) E. F. Etter, M. A. Kuhn, F. S. Fay, *J. Biol. Chem.* **1994**, *269*, 10141–10149.
- [5] a) H. M. Kim, B. R. Cho, *Acc. Chem. Res.* **2009**, *42*, 863–872; b) H. M. Kim, B. R. Cho, *Chem. Asian J.* **2011**, *6*, 58–69; c) S. Sumalekshmy, C. J. Fahrni, *Chem. Mater.* **2011**, *23*, 483–500.
- [6] *The Handbooks—A Guide to Fluorescent Probes and Labeling Technologies, 10th ed.* (Ed.: R. P. Haugland), Molecular Probes, Eugene, **2005**.
- [7] K. Gaus, E. Gratton, E. P. Kable, A. S. Jones, I. Gelissen, L. Kritharides, W. Jessup, *Proc. Natl. Acad. Sci. USA* **2003**, *100*, 15554–15559.
- [8] R. Y. Tsien, *Biochemistry* **1980**, *19*, 2396–2404.
- [9] K. A. Connors, *Binding Constants*, Wiley, New York, **1987**.
- [10] a) R. Y. Tsien, T. Pozzan, T. J. Rink, *J. Cell Biol.* **1982**, *94*, 325; b) R. Y. Tsien, T. Pozzan, *Methods Enzymol.* **1989**, *172*, 230–261; c) A. Takahashi, P. Camacho, J. D. Lechleiter, B. Herman, *Physiol. Rev.* **1999**, *79*, 1089–1125.
- [11] a) J. R. Long, R. S. Drago, *J. Chem. Educ.* **1982**, *59*, 1037–1039; b) K. J. Hirose, *Incl. Phenom. Macrocycl. Chem.* **2001**, *39*, 193–209.
- [12] a) S. Lin, K. A. Fagan, K. X. Li, P. W. Shaul, D. M. Cooper, D. M. Rodman, *J. Biol. Chem.* **2000**, *275*, 17979–17985; b) T. Nagai, S. Yamada, T. Tominaga, M. Ichikawa, A. Miyawaki, *Proc. Natl. Acad. Sci. USA* **2004**, *101*, 10554–10559.
- [13] J. N. Demas, G. A. Crosby, *J. Phys. Chem.* **1971**, *75*, 991–1024.
- [14] S. K. Lee, W. J. Yang, J. J. Choi, C. H. Kim, S. J. Jeon, B. R. Cho, *Org. Lett.* **2005**, *7*, 323–326.
- [15] C. Xu, W. W. Webb, *J. Opt. Soc. Am. B* **1996**, *13*, 481–491.

Received: February 15, 2011  
Published online: June 17, 2011